OXFORD

Human Molecular Genetics, 2022, Vol. 31, No. 3 399–409

https://doi.org/10.1093/hmg/ddab258
Advance Access Publication Date: 7 September 2021
General Article

GENERAL ARTICLE

Distinct functional classes of *PDGFRB* pathogenic variants in primary familial brain calcification

Sandrine Lenglez[1], Ariane Sablon[1], Gilles Fénelon[2], Anne Boland[3], Jean-François Deleuze[3], Claire Boutoleau-Bretonnière[4,5], Gaël Nicolas[6] and Jean-Baptiste Demoulin[1,*]

[1]De Duve Institute, Université catholique de Louvain, Brussels BE-1200, Belgium, [2]Department of Neurology, APHP, CHU Henri Mondor, Créteil F-94000, France, [3]Université Paris-Saclay, CEA, Centre National de Recherche en Génomique Humaine, Evry F-91057, France, [4]CHU Nantes, Centre Mémoire Ressource et Recherche (CMRR), Department of Neurology, Nantes F-44093, France, [5]Inserm CIC 04, Nantes F-4409, France and [6]Normandie University, UNIROUEN, Inserm U1245, CHU Rouen, Department of Genetics and CNR-MAJ, Rouen F-76000, France

*To whom correspondence should be addressed at: Jean-Baptiste Demoulin: Experimental Medicine Unit, UCLouvain, avenue Hippocrate 75, box B1.74.05, Brussels BE-1200, Belgium. Tel: +32 27646529; Fax: +32 27647430; Email: jb.demoulin@uclouvain.be and Gaël Nicolas: Department of Genetics and CNR-MAJ, Normandie Univ, UNIROUEN, Inserm U1245, CHU Rouen, FHU G4 Génomique, Rouen F-76000, France. Tel: +33 235148280; Fax: +33 235148237; Email: gaelnicolas@hotmail.com

Abstract

Platelet-derived growth factor receptor beta *(PDGFRB)* is one of the genes associated with primary familial brain calcification (PFBC), an inherited neurological disease (OMIM:173410). Genetic analysis of patients and families revealed at least 13 *PDGFRB* heterozygous missense variants, including two novel ones described in the present report. Limited experimental data published on five of these variants had suggested that they decrease the receptor activity. No functional information was available on the impact of variants located within the receptor extracellular domains. Here, we performed a comprehensive molecular analysis of *PDGFRB* variants linked to PFBC. Mutated receptors were transfected in various cell lines to monitor receptor expression, signaling, mitogenic activity and ligand binding. Four mutants caused a complete loss of tyrosine kinase activity in multiple assays. One of the novel variants, p.Pro154Ser, decreased the receptor expression and abolished binding of platelet-derived growth factor (PDGF-BB). Others showed a partial loss of function related to reduced expression or signaling. Combining clinical, genetic and molecular data, we consider nine variants as pathogenic or likely pathogenic, three as benign or likely benign and one as a variant of unknown significance. We discuss the possible relationship between the variant residual activity, incomplete penetrance, brain calcification and neurological symptoms. In conclusion, we identified distinct molecular mechanisms whereby *PDGFRB* variants may result in a receptor loss of function. This work will facilitate genetic counseling in PFBC.

Introduction

Primary familial brain calcification (PFBC, previously known as idiopathic basal ganglia calcification or Fahr disease) is a rare inherited neurological disorder characterized by bilateral calcification of basal ganglia and other brain regions (1). Affected individuals may exhibit a range of non-specific neuropsychiatric symptoms, including movement disorders, cognitive impairment and psychiatric manifestations. The disease has

Received: July 26, 2021. **Revised:** August 30, 2021. **Accepted:** August 31, 2021

been linked to heterozygous variants of four genes, which are transmitted in an autosomal dominant manner: *SLC20A2* [OMIM:158378], *XPR1* [OMIM:605237], *PDGFRB* [OMIM:173410] and *PDGFB* [OMIM:190040] (1–4). More recently, biallelic alterations causing PFBC were identified in *MYORG* [OMIM:618255] and *JAM2* [OMIM:606870] (5,6). Most of these genes contribute to the blood–brain barrier function, the alteration of which is key to PFBC pathophysiology (7). *SLC20A2*, *XPR1*, *MYORG* and *JAM2* encode two phosphate transporters, a glycosidase and a tight junction protein, respectively. *PDGFB* encodes platelet-derived growth factor-B, the ligand of the PDGFRB receptor tyrosine kinase, also named PDGF receptor β (PDGFRβ) (8). The PDGFB-PDGFRB axis plays a key role in pericyte development in multiple organs, including the brain (9). Homozygous deletion of *Pdgfb* or *Pdgfrb* is lethal in mice due to hemorrhages (9). A mouse model carrying a viable *Pdgfb* hypomorphic allele shows brain calcification (3). Accordingly, pathogenic *PDGFB* variants typically introduce a premature stop codon, suggesting that a loss of PDGFB-PDGFRB signaling may cause PFBC through haploinsufficiency (3).

PDGFRB encodes a cell surface receptor, which comprises five extracellular immunoglobulin-like domains (D1–D5), a transmembrane (TM) helix, an inhibitory juxtamembrane (JM) domain, a split tyrosine kinase domain (TKD) and a C-terminal tail (Fig. 1). PDGF binding to D2 and D3 induces the receptor dimerization and conformation change, which activates the intracellular TKD (8). The subsequent receptor phosphorylation triggers multiple signaling cascades, including MAP kinases, phosphatidylinositol-3 kinase, phospholipase Cγ and signal transducers and activators of transcription (STAT) factors. Overactivation of PDGF receptor β signaling due to somatic mutations is at the origin of several soft tissue and hematological malignancies (8,10). In addition, germline *PDGFRB* gain-of-function mutations were identified in rare inherited disorders with partial overlap: infantile myofibromatosis, Kosaki overgrowth syndrome, Penttinen premature aging syndrome and hereditary progressive mucinous histiocytosis (11,12).

In 2012, the first two *PDGFRB* variants were reported in PFBC patients: p.L658P, which co-segregated with the disease in a large pedigree, and p.R987W in a sporadic case (2). We and others showed that the p.L658P variant was devoid of kinase activity in various cellular assays (13–15). A number of additional *PDGFRB* variants were reported in patients with PFBC or related disorders (16–21). Most of these variants are missense and have not been functionally characterized. The goal of the present study was to establish their impact at the molecular level. In addition, we report two new *PDGFRB* variants in two sporadic PFBC cases, including the first PFBC patient with a confirmed *de novo PDGFRB* mutation. Using various cellular assays, we tested the activity of the PDGFRB mutants and showed that they belong to distinct functional classes according to their impact on the receptor expression, traffic to the cell surface, ligand binding and kinase activity.

Results

Novel and previously identified variants included in the study

The complete list of *PDGFRB* variants analyzed in the present study is shown in Table 1 and Figure 1. For simplicity, we will refer to each receptor mutant using the one letter amino acid code and the position of the substitution in the full-length receptor polypeptide. We first selected six variants that were reported in the literature in patients with PFBC and not experimentally characterized (M1?, R226C, R376W, P596L, G612R, D737N)

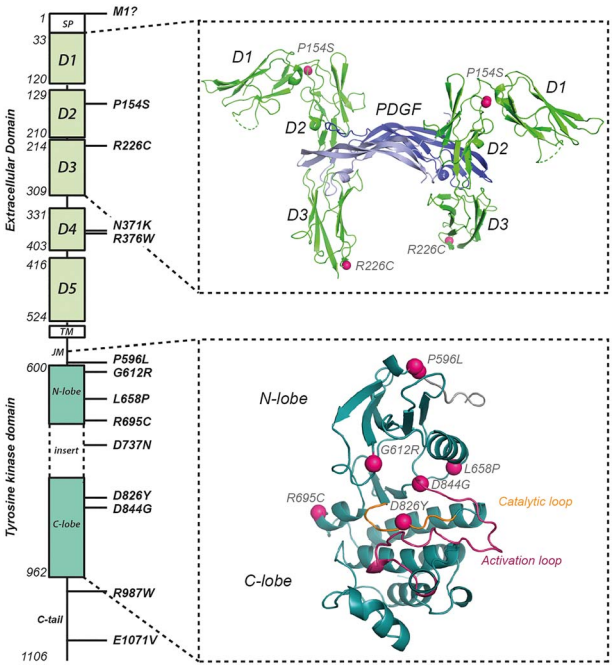

Figure 1. Localization of variants in the PDGFRB structure. The PDGFRB polypeptide includes a signal peptide (SP), five extracellular Ig-like domains (D1–D5), a transmembrane domain (TM), a juxtamembrane domain (JM), and an intracellular part composed of a split kinase domain and a C-terminal tail. The position of each receptor domain is based on UniProt. The structure of PDGFRB (D1–D3) complexed to PDGF-BB (in blue) was drawn using PyMOL (upper right panel, PDB reference 3MJG). The positions of the kinase domain mutations are shown in the highly conserved PDGFRA structure (lower right panel, PDB reference 5K5X).

(16,17,19). In comparison, we included three pathogenic or likely pathogenic variants that were previously investigated, namely L658P, R695C and D844G, as well as E1071V, for which conflicting results were published (13,14,21). We did not reanalyze R987W, for which ample experimental data are available (14,15,22). We also tested N371K, a variant of unknown significance reported in a patient with neurological symptoms in which the presence of calcification was not investigated (18). In addition, we report two novel *PDGFRB* substitutions in unpublished cases.

Clinical summaries of novel patients

Case EXT_1902. This 77-year-old man had a neurological follow-up for more than 12 years, in the context of a gait disorder with cognitive impairment and behavioral changes. Wide-based, unsteady gait was reported since the age of 27. The patient complained of progressive worsening from the age of 65. Upon examination, the patient showed axial cerebellar ataxia, slow walking with small steps, moderate limb and axial hypertonia, bradykinesia, marked dysarthria, but no tremor (motor part of the Unified Parkinson's Disease Rating Scale (UPDRS-III): 25/108). Although some degree of dopa-sensitivity was reported at the age of 65, an acute levodopa challenge test revealed no dopa-sensitivity at the age of 67. The patient developed a swallowing disorder and urinary incontinence. Minimental state examination scored 11/29 (One item was missing as the patient was not able to read the sentence.) Brain CT scan at 74 years showed extensive brain calcifications affecting lenticular and caudate nuclei, thalami, subcortical white matter, cortical regions, and the posterior fossa (cerebellar

Table 1. List of *PDGFRB* variants included in the present study

Variant	Nucleotide	Number of cases	Brain calcification	Neurological symptoms	Ref.
M1?	c.3G > A	3 (family)	Yes	Asymptomatic	(17)
P154S	c.460C > T	1	Yes	Parkinsonism, cognitive impairment, gait disorder	Novel
R226C	c.676C > T	1	Yes	Dyskinesia	(21)
N371K[a]	c.1113C > G	1	Unknown	Present	(18)
R376W[b]	c.1126C > T	2 (family)	1 of 2	Cognitive and motor dysfunction	(19)
P596L	c.1787C > T	1	Yes	Migraine	(21)
G612R	c.1834G > A	3 (family)	Yes	Paresthesia, epilepsy, anxiety, dizziness	(16)
L658P	c.1976T > C	13 (family)	Yes	Variable	(2)
R695C	c.2083C > T	2	1 of 2	Progressive supranuclear palsy	(14), Novel
D737N	c.2209G > A	2 (family)	Yes	None/dizziness	(17)
D826Y	c.2476G > T	1	Yes	Anxiety and attention deficit disorder	Novel
D844G	c.2531A > G	1	Yes	Sleepwalking	(21)
R987W	c.2959C > T	1	Yes	Parkinsonism, cognitive impairment, pyramidal tract signs	(2)
E1071V	c.3212A > T	1	Yes	Psychosis	(20)

[a]This patient was not diagnosed with PFBC.
[b]This variant was combined with a pathogenic CASR p.M811V variant in the patient with calcification and symptoms.

hemispheres and vermis) (Fig. 2A). Total Calcification Score (TCS) was 46 (20). Calcium-phosphorus blood assessment was normal. Genetic investigations consisted in whole exome sequencing with a focused interpretation on an *in silico* gene panel, showing the presence of a heterozygous c.460C > T, p.(Pro154Ser) *PDGFRB* variant, hereafter referred to as P154S. This variant was confirmed by Sanger sequencing. It was found once in the gnomAD database (23), and was predicted deleterious by Mutation Taster, SIFT, PolyPhen-2. His family originated from Portugal. He had a family history of gait disorder in his mother, with no further details available. DNA from relatives was not available for assessing the segregation of this variant.

Case 1975057. This 12-year-old girl was diagnosed with anxiety and attention deficit disorder. She also mentioned one episode of transient auditory hallucinations. In the context of cephalalgia, she underwent brain imaging. MRI showed hypointensities in susceptibility-weighted images (SWAN) in both lenticular nuclei as well as the left caudate head and the left cerebellar hemisphere while FLAIR-weighted images showed white matter hyperintensities, mostly in the periventricular regions, which were associated in some places to small cystic images (Fig. 2C). CT scan confirmed that the SWAN hypointensities were genuine calcifications (Images were not available to us for rating.) The CT scan report also mentioned, in addition to bilateral lenticular calcifications and punctate calcifications in the left cerebellar hemisphere, punctate calcifications in both thalami and cortex-white matter interface in the frontal lobe, bilaterally, with no description of calcified areas in the cystic-like lesions on MRI.

Genetic investigations included the sequencing of a large panel of genes by NGS (GeneDx), and mitochondrial mutations assessment. A heterozygous c.2476G > T, p.(Asp826Tyr) variant in the *PDGFRB* was identified, hereafter referred to as D826Y. Assessment of parental DNA showed that the mutation occurred *de novo* in the patient. This variant is absent from gnomAD and is predicted deleterious by Mutation Taster, SIFT and PolyPhen-2. In addition, low-level mosaicism for mitochondrial mutations unexpectedly revealed a m.3243A > G mutation in the *MT-TL1* mitochondrial gene (leucine tRNA 1 encoding gene), known as causing MELAS syndrome. It was present in 2% of the blood cells and was not retrieved in the mother's blood.

Patient EXT_481. This woman showed personality changes from the age of 52, followed by a speech disorder and behavioral troubles. Neuropsychological assessment revealed a moderate cognitive dysexecutive syndrome, later associated with memory and gnosis impairment. Physical examination was unremarkable. MRI showed frontal atrophy and CSF Alzheimer disease (AD) biomarkers showed elevated Tau protein (574 ng/l, $N < 350$), phosphorylated Tau (89, $N < 50$), with normal Aβ40 values (1151, $N > 500$) and an Aβ42/40 ratio close to the threshold (0.052, $N > 0.05$). A frontal form of AD was suspected despite an atypical profile of biomarkers and whole exome sequencing was performed in this context. She had a family history of late-onset dementia in her mother (onset >80 years). In exome data, no putatively pathogenic variant was found in the known Mendelian dementia genes including autosomal dominant AD genes (24). Her *APOE* genotype was 3–4, which is a moderate AD risk factor. Unexpectedly, we identified a heterozygous c.2083C > T, p.(Arg695Cys) in the *PDGFRB* gene. A CT scan performed at the age of 56 revealed no brain calcification (TCS = 0, Fig. 2B).

Biological activity of PDGFRB variants

We introduced mutations corresponding to each variant in a human HA-tagged *PDGFRB* cDNA. They were co-transfected with luciferase reporters that respond to MAP kinase-activated serum response factor (SRE) or STAT transcription factor (GRR5), as previously described (13). Stimulation of cells expressing the wild-type receptor with PDGF-BB increased the luciferase activity by about four-fold (Fig. 3). Eight mutants showed a significantly decreased activity upon stimulation in both luciferase assays. In addition, R695C had a significant impact in the GRR5 assay only. Altogether, 9 out of 13 mutants showed a loss of function of at least 30%. R376W, D737N and E1071V had a marginal effect in one assay, while N371K and E1071V increased the SRE reporter activity.

We further evaluated selected mutant receptors in Ba/F3 cells, a well-established model to test the ability of growth factor receptors to stimulate cell proliferation (22). Stable cell lines were produced by electroporation, selection of puromycin-resistant populations and sorting. The homogenous cell surface expression of the receptor was verified by flow cytometry (Fig. 4A). We noticed a reduced expression of P154S. Tritiated

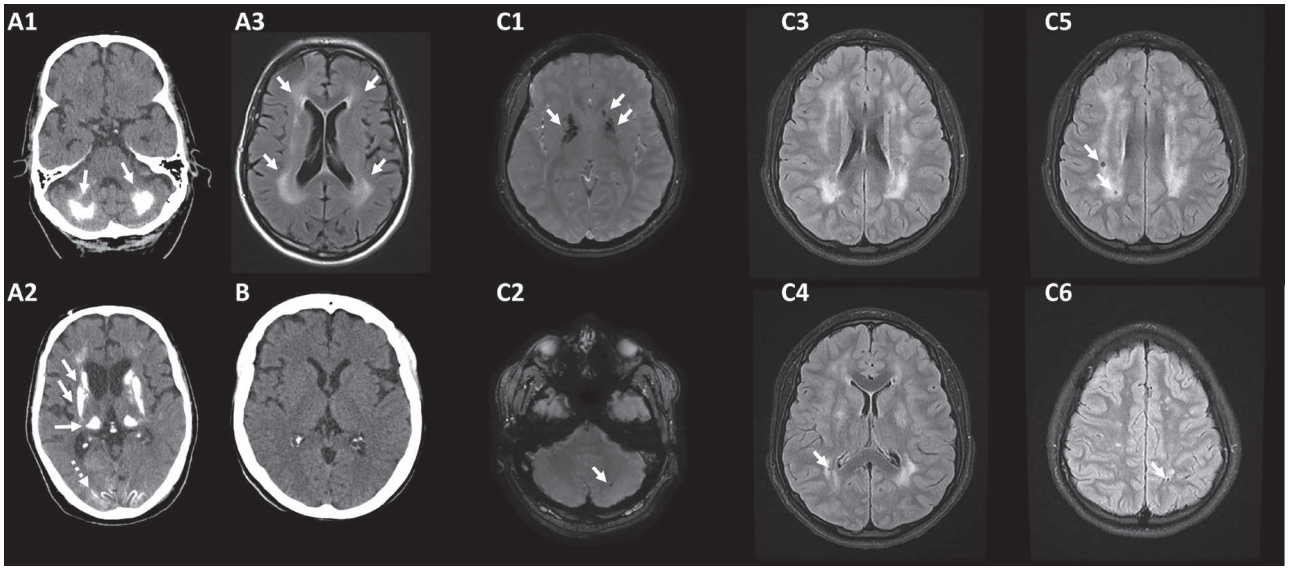

Figure 2. Brain imaging in patients EXT_1902, EXT_481 and 1975057. (**A1**, **A2**) Brain calcifications in patient EXT_1902 (P154S) on CT scan (axial views) in the cerebellar hemispheres (white arrows, A1) lenticular and caudate nuclei (oblique arrows, A2), thalami (horizontal arrow, A2), subcortical white matter, and occipital cerebral cortex (dotted arrow, A2). (**A3**) Brain MRI of patient EXT_1902 showing white matter hyperintensities (axial view, FLAIR, white arrows). (**B**) Absence of brain calcification in an R695C PDGFRB variant carrier (EXT_481) on CT scan. (**C1–C6**) Brain MRI of patient 1975057 (D826Y) showing lenticular, caudate and cerebellar calcifications on susceptibility-weighted images (SWAN, white arrows, C1, C2) and white matter hyperintensities with non-calcified cystic images (FLAIR, white arrows, C4–C6).

thymidine incorporation experiments confirmed that the P154S and G612R variants did not respond to PDGF-BB stimulation (Fig. 4B). R226C and P596L significantly decreased the response to PDGF-BB. N371K, R376W and D737N had a modest effect, which was not statistically significant. These observations confirmed the luciferase activity results. In conclusion, nine variants conferred a significant loss of function in our assays.

Mutant PDGFRB kinase activity

Seven mutations were located within the intracellular tyrosine kinase domain or in the vicinity (Fig. 1). We previously showed that L658P was devoid of kinase activity (13). Therefore, we tested whether they could alter the ability of the receptor to auto-phosphorylate upon overexpression in HEK 293T cells, using an anti-phosphotyrosine antibody in western blot experiments (Fig. 5). All variants were expressed at a detectable level. In multiple experiments, we did not observe any phosphorylation of G612R, D827Y and D844G, suggesting that these amino acid substitutions, like L658P, completely disrupted the PDGFRB kinase enzymatic activity (Fig. 5 and Supplementary Material, Fig. S1). The phosphorylation of P596L (located in the JM domain), was significantly reduced, indicating that this mutation could also perturb the kinase domain function. By contrast, D737N (in the insert) and the mutations located in the extracellular domain had no impact on the ability of the receptor to undergo ligand-independent autophosphorylation. Taken together, these results define a group of loss-of-function variants that disrupt the PDGFRB kinase activity.

PDGFRB cell surface expression and ligand binding

In Figure 5, the western blots show multiple bands resulting from differential glycosylation: the lighter receptor band corresponds to immature N-glycosylation in the endoplasmic reticulum (ER), while the upper heavy band represents mature fully glycosylated receptor, which is present at the cell surface (25). Several mutants, particularly P154S and R226C, showed a decreased level of mature receptor, suggesting a perturbation of glycosylation and/or traffic from the ER to the plasma membrane.

To explore this possibility further, in particular for extracellular mutants, we performed flow cytometry on transiently transfected HEK 293T cells and stably transfected Ba/F3 cells (Fig. 6A and B). The quantification of multiple experiments showed that the cell surface expression of M1?, P154S and R226C was consistently decreased in both cell types, suggesting a defect in the receptor biosynthesis and/or traffic to the cell surface. The decrease in P154S expression could not explain the complete lack of activity in cellular assays. Since the P154 residue is located in the receptor ligand-binding domain (Fig. 1), we tested whether the P154S substitution could affect ligand binding. To do so, we produced luminescent PDGF-BB by fusing the sequences of PDGFB and nano-luciferase (PDGF-nLUC). This tracer specifically bound to cells transfected with the wild-type receptor, either HEK 293T or Ba/F3 cells (Fig. 6C and D), but not to mock-transfected cells. To further demonstrate the specificity of this assay, we showed that cells did not bind to a secreted nano-luciferase control (fnLUC). Cells transfected with the P154S mutant did not bind to PDGF-nLUC. The R226C mutant showed a decreased ability to bind to PDGF-nLUC, which could not be entirely explained by its decreased expression at the cell surface. By contrast, M1? N371K and R376W showed PDGF-nLUC binding capacities related to their expression levels. In conclusion, we demonstrate amino-acid substitutions in the extracellular domains affect the receptor cell surface expression and ligand binding.

Discussion

Among the 13 *PDGFRB* variants associated with PFBC, 10 showed a significant loss of function (Table 2). In five cases, our results were consistent with previous publications (13–15,21). Importantly, our investigations revealed novel mechanisms of receptor inactivation.

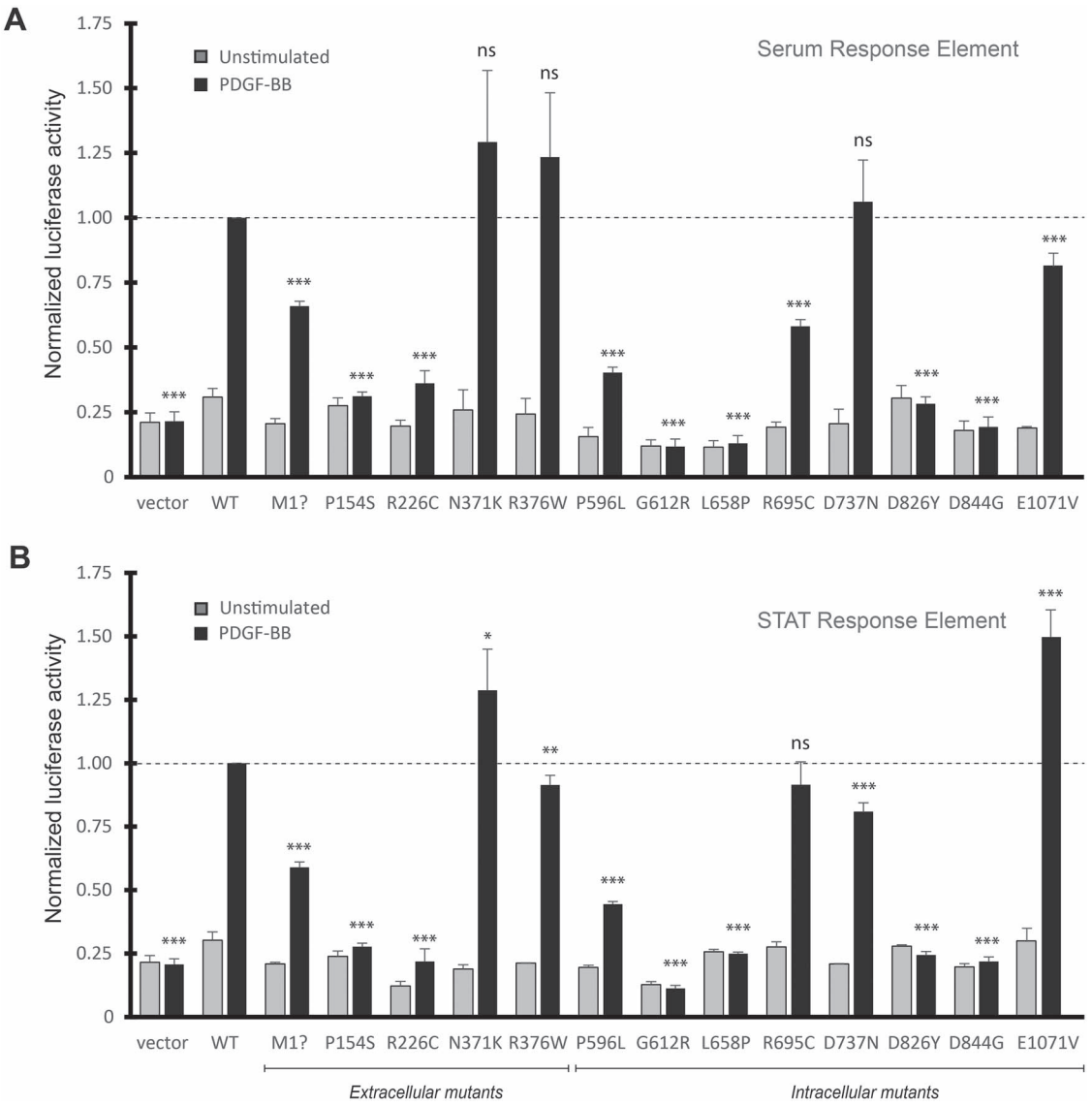

Figure 3. Loss of signaling activity of PDGFRB variants associated with PFBC. PAE cells were transiently transfected with the indicated mutant receptor, a β-galactosidase control plasmid and a luciferase reporter that is responsive to MAP kinases (SRE, **A**) or STAT transcription factors (GRR5, **B**). Cells were stimulated or not with PDGF-BB (25 ng/ml) for 24 h. Results were normalized using the wild-type receptor as a reference. The average of at least three experiments is shown with SEM.

Four TKD variants resulted in a complete loss of tyrosine kinase enzymatic activity: G612R, L658P, D826Y and D844G. These variants affected key conserved residues that are located in the catalytic cleft (Fig. 1). In particular, D844 belongs to the Asp-Phe-Gly motif in the activation loop that is essential for kinase activity. An additional TKD mutant, R695C, had a partial effect on receptor autophosphorylation and is further discussed below. The P596L substitution in the JM domain also reduced the kinase activity. This was unexpected since all *PDGFRB* somatic and germline JM mutations characterized so far have the opposite effect: they activate the receptor and are typically associated with Kosaki overgrowth syndrome, infantile myofibromatosis or fusiform aneurysms (10,11).

We identified the inability to bind to PDGF-BB as a second mechanism leading to a loss of receptor function. Binding to PDGF-BB was abolished by the P154S mutation, and reduced by R226C. These two residues do not directly interact with the ligand (Fig. 1). Instead, the two mutations are likely to disrupt the conformation of the receptor ligand-binding domain. In addition, both mutant receptors showed a variable decrease in cell surface expression, which represents a third mechanism of receptor inactivation. The M1? variant was also associated with slightly reduced cell surface expression. This mutation is predicted to shift the translation start codon to the second methionine at position 7, which is associated with a different Kozak sequence (GCGATGC instead of ACCATGC). This may in theory affect the translation efficiency, although this was not confirmed by prediction algorithms such as NetStart 1.0 (26). Importantly, according to SignalP 4.1, this change does not affect the signal peptide cleavage site (27).

Our results allowed a reclassification of variants according to the ACMG-AMP recommendations, mostly by using the PS3 criterion: evidence for an *in vitro* loss-of-function effect in the context of PDGFRB-related PFBC (Table 2) (28). We propose the reclassification of 5 variants of unknown significance (class 3, based on the strict application of the ACMG-AMP criteria),

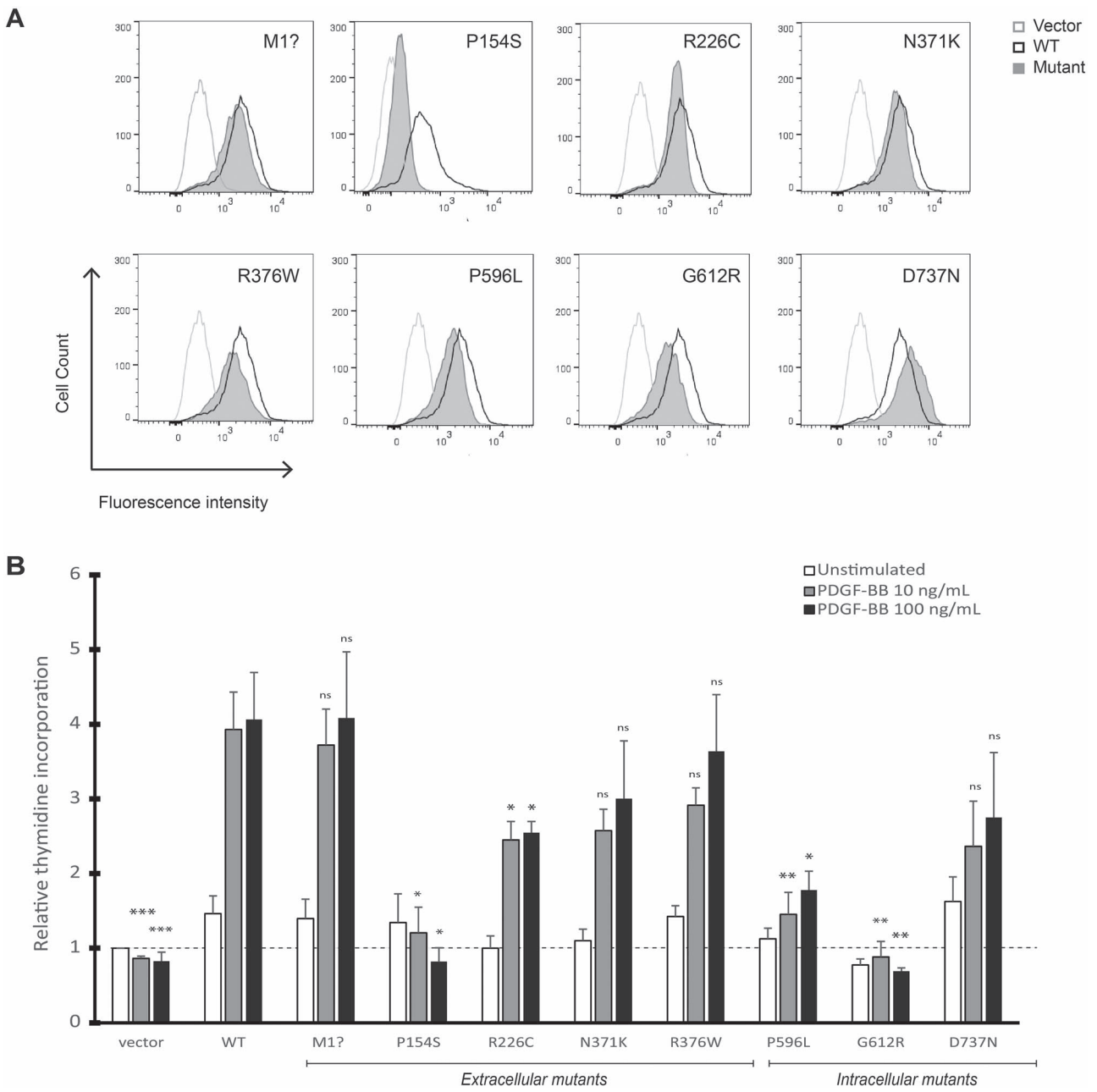

Figure 4. Decreased mitogenic activity of PFBC-associated variants. (**A**) Ba/F3 cells were stably transfected with the indicated HA-tagged receptor mutant and sorted. Receptor expression was analyzed by flow cytometry using an anti-HA antibody coupled to APC. (**B**) Cells were washed, seeded in microtiter plates and stimulated with control medium, interleukin-3 or PDGF-BB (10 or 100 ng/ml) for 24 h. Tritiated thymidine was added to each well 4 h before cell harvest. The radioactivity incorporated into DNA is shown (average of at least three experiments, with SEM). Statistical analyses compare mutant cells to wild-type controls (with the same treatment). All cell lines responded similarly to interleukin-3, used as positive control (data not shown).

namely M1?, P154S, R226C, P596L, G612R, into class 4 (likely pathogenic), enabling their use for genetic counseling (Table 2). Indeed, at the time of genetic screening of patient EXT_1902, variant P154S was rated as class 3, despite extreme low frequency in gnomAD (one carrier, PM2) and *in silico* predictions of deleteriousness (PP3). Similarly, R226C and P596L are absent or extremely rare in gnomAD (PM2), are predicted damaging by *in silico* tools (PP3), and were identified in a single patient. The M1? variant was present in three asymptomatic individuals with non-ambiguous brain calcifications and absent in one relative with a normal CT scan (17). In the ACMG-AMP recommendations, variants affecting the initiation codon may be automatically classified as null variants, providing a very strong argument for pathogenicity (PVS1). However, this may not automatically apply here, because of the putative alternative in-frame start codon, as discussed above. Therefore, despite a supporting co-segregation argument (PP1), we initially considered it as a class 3 variant (based on PM2, PP1, PP3). Our experimental results support a reclassification of these five variants as likely pathogenic. The PS3 argument can also apply to the D826Y variant, which already belonged to class 4 due to its *de novo* occurrence (PS2), and can now considered as pathogenic (class 5).

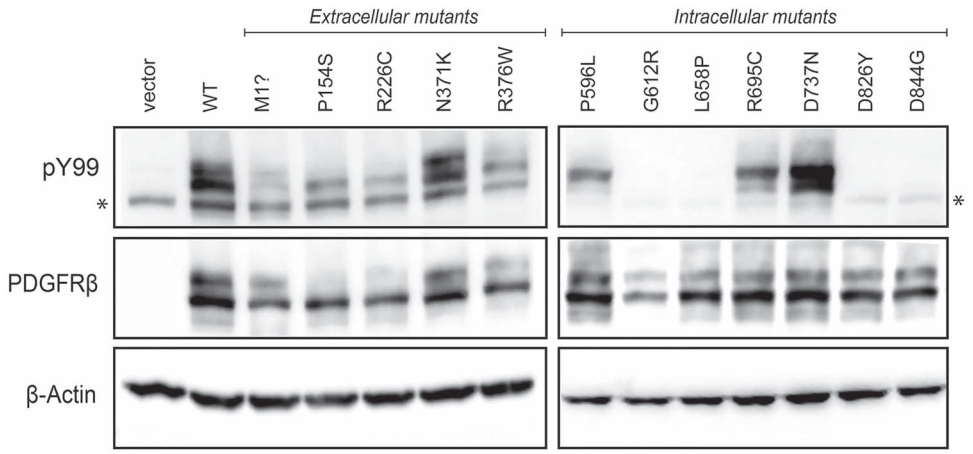

Figure 5. Identification of kinase-dead PDGFRB mutants. HEK 293T cells were transiently transfected with the indicated receptor. After 24 h, cell lysates were analyzed by western blot using anti-phosphotyrosine (PY99), anti-PDGFRB and anti-β-actin antibodies. One representative experiment out of three is shown. Result quantification is shown in Supplementary Material, Figure S2. The asterisk indicates a nonspecific band.

Table 2. Summary of the functional analyses of 13 *PDGFRB* variants associated with PFBC

Variant	Expression	Ligand binding	Kinase activity	Signaling	Prior clinical significance	Proposed novel clinical significance	Ref.
M1?	Decreased	–	–	Decreased	Unknown significance[a]	Likely pathogenic	–
P154S	Decreased	Lost	–	Lost	Unknown significance	Likely pathogenic	–
R226C	Decreased	Decreased	–	Decreased	Unknown significance	Likely pathogenic	–
R376W	–	–	–	–	Unknown significance	Likely benign	–
P596L	–	–	Decreased	Decreased	Unknown significance	Likely pathogenic	–
G612R	–	–	Lost	Lost	Unknown significance	Pathogenic	–
L658P	–	–	Lost	Lost	Pathogenic	Pathogenic	(13,15)
R695C	Decreased	–	–	Decreased	Likely pathogenic	Unknown significance	(14)
D737N	–	–	–	–	Unknown significance	Likely benign	–
D826Y	–	–	Lost	Lost	Likely pathogenic	Pathogenic	–
D844G	–	–	Lost	Lost	Pathogenic	Pathogenic	(21)
R987W	Decreased	–	Decreased	Decreased	Likely pathogenic	Likely pathogenic	(13–15)
E1071V	–	–	–	–	Unknown significance	Likely benign	(13,15)

The proposed clinical significance of the variants is based on experimental results of the present study and previous reports (with references) according to the criteria of ACMG-AMP (28). We did not re-evaluate R987W. See discussion for details.
[a]Although the variant could be automatically rated as pathogenic given the initiation codon loss argument (PVS1), the existence of an in-frame putative translation initiation site at codon 7 should warn against automatic use of the PVS1 criterion in this case, thus leading to a variant of unknown significance.
[b]Although the authors rated this variant as likely pathogenic in the primary report, strictly using ACMG-AMP recommendations would lead to a variant of unknown significance classification (class 3) prior to functional analyses: PM2 (absent in controls), PP1 (segregation, supporting argument: two informative meioses), PP3 (*in silico* predictions).

By contrast, our results question the pathogenicity of R695C, previously considered as likely pathogenic. Our experimental results and previous reports suggest that R695C has mild effects on PDGFRB functions (14). This substitution had been previously reported in a single 83-year-old patient with neurological symptoms and macroscopic calcifications at autopsy (14). Absence of brain calcification on the CT scan of the 53-year-old case reported here suggests that this variant might be associated with incomplete penetrance (BS2). Indeed, the age of 50 is usually considered as a threshold for full penetrance of brain calcifications on CT scan for PFBC. In addition, this variant has a higher occurrence in genome databases (32/282736 alleles in gnomAD) than all other pathogenic variants (BS1). Altogether, R695C is associated with contradictory benign and pathogenic criteria, pointing to a variant unknown significance.

Three variants, namely R376W, D737N and E1071V, did not present any significant functional defect when introduced in our cellular assays. R376W was identified in a single patient who carried a *CASR* p.M811V clinically relevant variant, which seems sufficient to explain the observed phenotype (19). Hence, the R376W can also be classified as likely benign (19).

In a previous report, we showed that the E1071V mutation increased the receptor activity (13), which we subsequently confirmed in Ba/F3 cells (unpublished data) and in Figure 3B, suggesting that this variant, identified in a single patient, is likely benign. By contrast, Vanlandewijck and colleagues reported a slightly decreased phosphorylation of phospholipase Cγ by the E1071V mutant receptor (15). Whether this effect is sufficient to explain the PFBC phenotype is not clear.

We did not reanalyze the likely pathogenic R987W variant, which several investigators had extensively characterized before, demonstrating a partial loss of function (13–15). We have shown that the R987W mutation affects the receptor trafficking, leading to increased internalization and degradation (13). This defect is associated with a specific reduction in

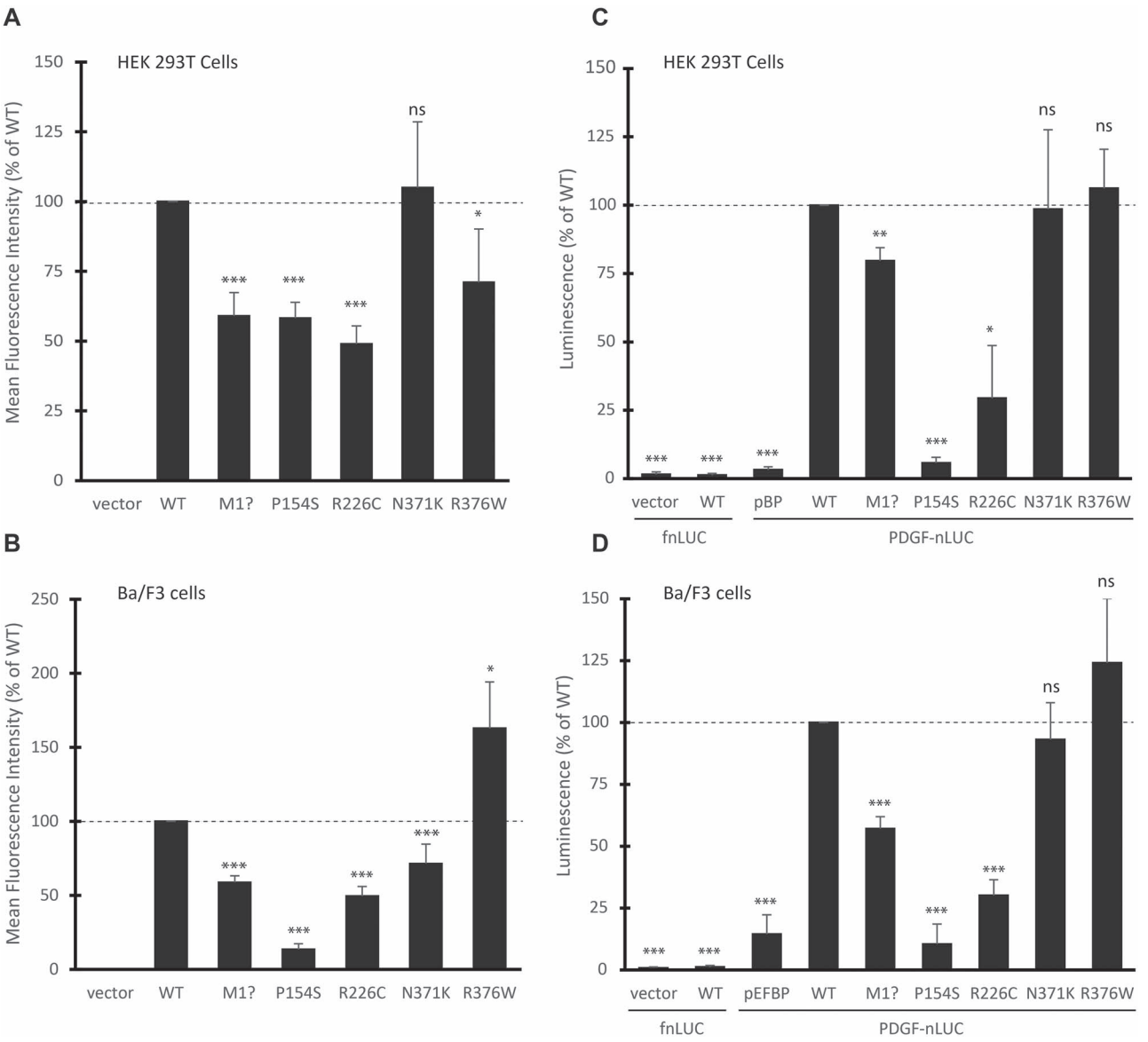

Figure 6. Impaired cell surface expression and ligand binding. (**A**) HEK 293T were transiently transfected with the indicated HA-tagged receptor mutant, as described in Figure 5. (**B**) Stable Ba/F3 cell lines are described in Figure 4. (**A** and **B**) Intact cells were stained with anti-HA antibody coupled to APC or PE and analyzed by flow cytometry. The mean fluorescence intensity was measured for each mutant and presented as a percentage of the WT signal. The average of at least five experiments is shown with SEM. (**C** and **D**) Cells were incubated with a PDGF-nLUC fusion or an fnLUC control for 45 min on ice. Cells were extensively washed and luminescence was measured in the presence of coelenterazine. The average of at least three experiments is shown.

STAT3 activation and phospholipase Cγ phosphorylation, suggesting a distinct mechanism of receptor inactivation in PFBC.

The D737N was detected in an asymptomatic 67-year-old mother and her 45-year-old son with mild pallidum calcifications and minor neurological symptoms (a one-year history of dizziness) (17). It is present at a very low frequency in gnomAD and is located in the TKD insert, which is not essential for kinase activity but recruits various signaling proteins to the receptor (8). Interestingly, the D737 residue is replaced by an asparagine in the otherwise highly conserved sequence of PDGF receptor α (PDGFRA), suggesting that the D737N substitution is unlikely to severely affect the receptor function. We suggest that this variant is likely benign, although we cannot exclude a subtle effect on PDGFRB activity.

Collectively, this study underlines the importance of a thorough experimental characterization of variants to complement clinical data and *in silico* predictions. Our results on R695C, D737N, and, to some extent, the M1? variant, also raise the question of the degree of loss of function required to result in brain calcification by the age of 50. The question of symptoms is even more complicated, given the weak correlation between the extent of calcifications and the symptomatic status (29).

Finally, we described two novel PFBC cases with *PDGFRB* variants and novel clinical features. Patient EXT_1902 showed particularly extensive brain calcification that included cortical calcifications, which, to our knowledge, were not reported before in *PDGFRB* pathogenic variant carriers (29). Of note, the D826Y variant, another complete loss-of-function variant associated with an early onset, is the first confirmed *de novo PDGFRB* mutation

in the context of PFBC. This patient showed a rather uncommon imaging presentation with cystic leukoencephalopathy associated to brain calcifications. She was also a carrier, at a very low level, of a mitochondrial mutation. However, it remains unclear whether this mutation contributed to the clinical and imaging features of this patient.

In conclusion, our study sheds light on the mechanisms leading to *PDGFRB* loss of function in PFBC. Our results also strongly support the pathogenicity of nine PFBC-associated variants, including two novel ones. This will facilitate the diagnosis of PFBC and interpretation of medical genetic results.

Materials and Methods

Selection of PDGFRB variants

We focused on *PDGFRB* variants identified in patients with brain calcifications and/or neurological symptoms (variants identified in the context of infantile myofibromatosis, Kosaki overgrowth syndrome and Penttinen premature aging syndrome were not included). Variants were selected following a literature search. We added two novel variants identified in the context of genetic screening for diagnostic purposes. We also report one patient with probable Alzheimer disease (AD) exhibiting a *PDGFRB* variant currently classified as likely pathogenic and incidentally identified upon exome sequencing for etiological assessment of early-onset probable AD. Patients provided informed written consent for genetic analyses. *PDGFRB* screening was performed by whole exome sequencing (CNRGH, Evry, France), or a large gene panel (so-called clinical exome, GeneDx). Clinical and brain imaging information was retrieved from patient medical charts.

Cell culture, plasmids and reagents

Human embryonic kidney (HEK) 293T cells and porcine aortic endothelial (PAE) cells were cultured in Dulbecco's modified Eagle's medium (DMEM, Lonza #BE12-741F) supplemented with 10% fetal calf serum (FCS) and 1% (100 U/ml) penicillin–streptomycin (Thermo #15140-122). Ba/F3 cells were cultured in the same medium supplemented with CHO cell supernatant containing interleukin-3, as described earlier (30).

PDGFRB (NM_002609.4) inserted into pEF-Bos-Puro (with a N-terminal HA tag) was used as a template for mutagenesis, using the Quikchange II XL kit (Agilent) with specific oligonucleotides described in Supplementary Material, Table S1 (Eurogentec, Belgium). All constructs were confirmed by Sanger sequencing (Eurofins).

Cell transfection

HEK 293T cells were transiently transfected essentially as described (31). Cells were seeded in 6-well plates (500 000 cells/well) and transfected the next day using the calcium phosphate method. DNA (3 μg in 90 μl of water) was mixed with 100 μl BBS Buffer (50 mM BES; 280 mM NaCl; 13.5 mM NaH_2PO_4, 1.5 mM Na_2HPO_4). $CaCl_2$ (2.5 M; 10 μl) was added. The solution was incubated for 20 min at room temperature. Precipitates were added to each well in the presence of 2 ml of medium with 10% FCS. After 4 h, cells were incubated in fresh medium overnight at 37°C. Cells were then washed with PBS and used for flow cytometry or western blot experiments.

Ba/F3 cells were stably transfected by electroporation (200 V, 1300 μF, 75 Ω) in a 4 mm cuvette (Eurogentec #CE-0004-50) with 40 μg of plasmid DNA and selected with puromycin (Sigma, 1 μg/ml) for 7 days. Cells were then sorted by flow cytometry to remove PDGFRB-negative cells, as described below.

Flow cytometry

One million cells (HEK 293T or Ba/F3) were harvested, washed and stained with anti-HA.11 antibody coupled to phycoerythrin (PE) or APC (1/100, Biolegend #901517 and #901523) in cell resuspension solution (PBS with 1 mM EDTA and 3% heat-inactivated serum) for 20 min at 4°C. Cells were washed, resuspended in cell resuspension solution, and analyzed using FACSVerse (BD Biosciences) to monitor the receptor cell surface expression. Ba/F3 cells were sorted using FACSAriaIII (BD Biosciences) to produce stable cell lines expressing homogenous levels of receptor. The PE fluorochrome was detected using a blue laser (488 nm) and 586 nm filter. A red laser (640 nm) combined with a 660 nm filter was used to detect APC. Similar results were obtained with the two fluorophores. Data was analyzed using the FlowJo software. Debris and dead cells were excluded from the analysis by appropriate gating based on side and forward scatter signals.

Western blot

Cells were lysed in lysis buffer (25 mM TRIS–HCl; 150 mM NaCl; 6 mM EDTA; 10% glycerol; 1% Triton X-100; pH 7.4; 1 μg/ml aprotinin; 1 mM Pefabloc and 1 mM sodium orthovanadate) for 30 min on ice and centrifuged at maximal speed to eliminate cellular debris for 10 min at 4°C. Protein concentrations were measured using the BCA protein assay kit (Thermo). Protein extracts (30 μg) were diluted in Laemmli sample buffer 4× (0.2 M Tris–HCl pH 6.8; 277 mM SDS; 6 mM bromophenol blue; 44.4% glycerol; 10% 2-mercaptoethanol) and loaded in Tris–glycine 4–12% Novex precast gels (Thermo). Electrophoresis was performed in a Mini Gel Tank (Thermo) in TRIS-glycine running buffer (25 mM Tris; 0.2 M glycine; 0.1% SDS). Proteins were transferred to Hybond P PVDF membranes (Amersham), using a Power Blotter XL (Thermo) in transfer buffer (50 mM TRIS; 42 mM glycine; 20% methanol). Membranes were blocked in 5% fat-free milk in TBS-T (20 mM TRIS; 137 mM NaCl; 0.1% Tween20) or in Odyssey Blocking Buffer (Licor) for 1 h at room temperature. Membranes were then incubated overnight at 4°C with antibodies of interest diluted in 5% bovine serum albumin (BSA): anti-β-actin (1/2000, Sigma #A5441), anti-PDGFRβ (1/1000, Cell Signaling #3169) or anti-pY99 (1/500, Santa Cruz #SC-7020). The day after, membranes were washed with TBS-T and incubated with secondary anti-rabbit-IgG antibodies coupled to horseradish peroxidase (HRP) (Cell Signaling #7074) or anti-mouse-IgG-HRP (Cell Signaling #7076) diluted at 1/5000 in TBS-T for 1 h at room temperature. After three successive washes, proteins were detected with Super-Signal West Pico chemiluminescent substrate (Thermo #34580). Images were captured with Fusion Solo S Western Blot Imager (Vilber) and analyzed with the Fusion Edge software (Vilber). Membranes were stripped in 0.4 M NaOH for 8 min prior to re-probing with a second antibody.

Luciferase reporter assay

PAE cells were seeded in duplicates in 24-well plates (50 000 cells/well). The next day, cells were transfected with 250 ng of pDRIVE-chEF1/RU5-LacZ (control β-galactosidase reporter, Invitrogen), 250 ng of wild-type or mutant HA-PDGFRB in pEF-Bos-Puro, 250 ng of luciferase reporter [driven by two serum-response elements (SRE) or five interferon-gamma response regions (GRR5), as described (13)], and 2 μl of Turbofect reagent

(Thermo #R0532) in 100 μl Opti-MEM (Thermo #31985047). Four hours after transfection, cells were washed with PBS, starved in DMEM without serum, stimulated or not with PDGF-BB (Peprotech #100-14B) at 25 ng/ml and incubated overnight at 37°C. Cells were washed with PBS and lysed in 100 μl passive lysis buffer (25 mM Tris-phosphate (pH 7.8); 2 mM DTT; 2 mM 1,2-diaminocyclohexane-N,N,N′,N′-tetraacetic acid; 10% glycerol; 1% Triton X-100) for 20 min at room temperature under agitation. Cell lysates (40 μl) were transferred in a 96-well plate with 40 μl of β-galactosidase substrate solution (165 mM Na_2HPO_4, 38 mM NaH_2PO_4, 2 mM $MgCl_2$, 0.5% 2-mercaptoethanol, 4.4 mM o-nitrophenyl-β-D-galacto-pyranoside). After 30 min at 37°C, the absorbance was measured at 405 nm using a Glomax Discover microplate reader (Promega). In parallel, 20 μl of cell lysates were transferred in a white 96-well plate with 50 μl of luciferase reagent (Promega #E1483). Luminescence was measured using a Glomax Discover microplate reader (Promega).

[^{3}H]-Thymidine incorporation assay

Ba/F3 cells were washed three times with DMEM to remove IL-3 from medium. Cells were seeded in a 96-well plate (20 000 cells per well in 200 μl) with or without interleukin-3 or PDGF-BB in quadruplicates, and incubated overnight at 37°C. After 20 h, 20 μl (0.02 Ci) of [methyl-^{3}H]-thymidine (Perkin Elmer #NET027X005MC) were added in each well and incubated at 37°C for 4 h. Cells were harvested in GF/C glass fiber filter-bottom 96-well microplates (Perkin Elmer #6005174) and dried at 55°C for 30 min. Scintillation liquid (40 μl, MicroScint-O, PerkinElmer) was added to each well and the incorporated tritium was measured using a TopCount instrument (Perkin Elmer).

PDGF binding assay

The PDGF-BB complete coding sequence (NM_002608_3) was amplified by PCR using specific oligonucleotides (Supplementary Material, Table S1) flanked by EcoRI and XbaI restriction sites. After digestion, the product was cloned in the pNLF1-C plasmid in frame with the nano-luciferase (nLUC) sequence (Promega), and verified by Sanger sequencing. HEK 293T were transfected with the PDGFB-nLUC construct using the calcium phosphate method. The supernatant was harvested after 24–48 h, filtered, centrifuged, aliquoted and stored at −20°C. As a control, we used a construct containing the signal peptide of the erythropoietin receptor in front of nLUC to produce secreted free nLUC (fnLUC, a kind gift from Stefan Constantinescu and Thomas Balligand, Ludwig Institute for Cancer Research, Brussels, Belgium). Supernatants containing equal luminescence levels of fnLUC or PDGFB-nLUC were added to 500 000 Ba/F3 cells, in 500 μl of medium. Cells were incubated for 45 min on ice to prevent PDGFRB internalization. After three washes with cold PBS, cells were resuspended in 500 μl of PBS. Cell suspension aliquots (50 μl) were transferred into a white 96-well plate with 50 μl of native coelenterazine (8 μg/ml, NanoLight #303-5). Luminescence was measured using a Glomax Discover microplate reader.

Statistical analysis

Experiments were reproduced three times for each mutant and normalized using the wild-type receptor as reference. The average of at least three experiments is shown with SEM. Statistical significance was assessed using a bilateral Student's *t*-test (***$P < 0.001$; **$P < 0.01$; *$P < 0.05$).

Supplementary Material

Supplementary Material is available at *HMGJ* online.

Acknowledgements

We are grateful to Nicolas Dauguet for technical support. A.S. is the recipient of a fellowship from FSR-FNRS. We thank Stefan Constantinescu and Thomas Balligand for generous donation of reagents. We are grateful to patient 1975057 and her family for contributing to the study. Collaboration CEA-DRF-Jacob-CNRGH—CHU de Rouen.

Conflict of Interest statement. None declared.

Funding

Actions de Recherche Concertées (ARC16/21-073 to J.B.D.); the French National Research Agency (CALCIPHOS, ANR-17-CE14-0008-02 to G.N.); European Regional Development Fund (European Union and Région Normandie; Europe gets involved in Normandy, (Recherche Innovation Normandie, RIN 2018 to G.N.); Fonds de la Recherche Scientifique - FNRS (grant AR836, to A.S.).

References

1. Westenberger, A., Balck, A. and Klein, C. (2019) Primary familial brain calcifications: genetic and clinical update. *Curr. Opin. Neurol.*, **32**, 571–578.
2. Nicolas, G., Pottier, C., Maltete, D., Coutant, S., Rovelet-Lecrux, A., Legallic, S., Rousseau, S., Vaschalde, Y., Guyant-Marechal, L., Augustin, J. *et al.* (2013) Mutation of the PDGFRB gene as a cause of idiopathic basal ganglia calcification. *Neurology*, **80**, 181–187.
3. Keller, A., Westenberger, A., Sobrido, M.J., Garcia-Murias, M., Domingo, A., Sears, R.L., Lemos, R.R., Ordonez-Ugalde, A., Nicolas, G., da Cunha, J.E. *et al.* (2013) Mutations in the gene encoding PDGF-B cause brain calcifications in humans and mice. *Nat. Genet.*, **45**, 1077–1082.
4. Legati, A., Giovannini, D., Nicolas, G., Lopez-Sanchez, U., Quintans, B., Oliveira, J.R., Sears, R.L., Ramos, E.M., Spiteri, E., Sobrido, M.J. *et al.* (2015) Mutations in XPR1 cause primary familial brain calcification associated with altered phosphate export. *Nat. Genet.*, **47**, 579–581.
5. Yao, X.P., Cheng, X., Wang, C., Zhao, M., Guo, X.X., Su, H.Z., Lai, L.L., Zou, X.H., Chen, X.J., Zhao, Y. *et al.* (2018) Biallelic mutations in MYORG cause autosomal recessive primary familial brain calcification. *Neuron*, **98**, 1116–1123 e1115.
6. Schottlaender, L.V., Abeti, R., Jaunmuktane, Z., Macmillan, C., Chelban, V., O'Callaghan, B., McKinley, J., Maroofian, R., Efthymiou, S., Athanasiou-Fragkouli, A. *et al.* (2020) Bi-allelic JAM2 variants lead to early-onset recessive primary familial brain calcification. *Am. J. Hum. Genet.*, **106**, 412–421.
7. Betsholtz, C. and Keller, A. (2014) PDGF, pericytes and the pathogenesis of idiopathic basal ganglia calcification (IBGC). *Brain Pathol.*, **24**, 387–395.
8. Demoulin, J.B. and Essaghir, A. (2014) PDGF receptor signaling networks in normal and cancer cells. *Cytokine Growth Factor Rev.*, **25**, 273–283.
9. Andrae, J., Gallini, R. and Betsholtz, C. (2008) Role of platelet-derived growth factors in physiology and medicine. *Genes Dev.*, **22**, 1276–1312.
10. Dachy, G., De Krijger, R.R., Fraitag, S., Theate, I., Brichard, B., Hoffman, S.B., Libbrecht, L., Arts, F.A., Brouillard, P., Vikkula,

M. et al. (2019) Association of PDGFRB mutations with pediatric myofibroma and myofibromatosis in 69 cases: implications for diagnosis and targeted therapy. *JAMA Dermatol.*, **155**, 946–950.
11. Guerit, E., Arts, F., Dachy, G., Boulouadnine, B. and Demoulin, J.B. (2021) PDGF receptor mutations in human diseases. *Cell. Mol. Life Sci.*, **78**, 3867–3881.
12. Onoufriadis, A., Boulouadnine, B., Dachy, G., Higashino, T., Huang, H.Y., Hsu, C.K., Simpson, M.A., Bork, K., Demoulin, J.B. and McGrath, J.A. (2021) A germline mutation in the platelet-derived growth factor receptor beta gene may be implicated in hereditary progressive mucinous histiocytosis. *Br. J. Dermatol.*, **184**, 967–970.
13. Arts, F.A., Velghe, A.I., Stevens, M., Renauld, J.C., Essaghir, A. and Demoulin, J.B. (2015) Idiopathic basal ganglia calcification-associated PDGFRB mutations impair the receptor signalling. *J. Cell. Mol. Med.*, **19**, 239–248.
14. Sanchez-Contreras, M., Baker, M.C., Finch, N.A., Nicholson, A., Wojtas, A., Wszolek, Z.K., Ross, O.A., Dickson, D.W. and Rademakers, R. (2014) Genetic screening and functional characterization of PDGFRB mutations associated with basal ganglia calcification of unknown etiology. *Hum. Mutat.*, **35**, 964–971.
15. Vanlandewijck, M., Lebouvier, T., Andaloussi Mae, M., Nahar, K., Hornemann, S., Kenkel, D., Cunha, S.I., Lennartsson, J., Boss, A., Heldin, C.H. et al. (2015) Functional characterization of germline mutations in PDGFB and PDGFRB in primary familial brain calcification. *PLoS One*, **10**, e0143407.
16. Mathorne, S.W., Sorensen, K., Fagerberg, C., Bode, M. and Hertz, J.M. (2019) A novel PDGFRB sequence variant in a family with a mild form of primary familial brain calcification: a case report and a review of the literature. *BMC Neurol.*, **19**, 60.
17. Wang, C., Yao, X.P., Chen, H.T., Lai, J.H., Guo, X.X., Su, H.Z., Dong, E.L., Zhang, Q.J., Wang, N. and Chen, W.J. (2017) Novel mutations of PDGFRB cause primary familial brain calcification in Chinese families. *J. Hum. Genet.*, **62**, 697–701.
18. Yavarna, T., Al-Dewik, N., Al-Mureikhi, M., Ali, R., Al-Mesaifri, F., Mahmoud, L., Shahbeck, N., Lakhani, S., AlMulla, M., Nawaz, Z. et al. (2015) High diagnostic yield of clinical exome sequencing in middle eastern patients with Mendelian disorders. *Hum. Genet.*, **134**, 967–980.
19. DeMeo, N.N., Burgess, J.D., Blackburn, P.R., Gass, J.M., Richter, J., Atwal, H.K., van Gerpen, J.A. and Atwal, P.S. (2018) Co-occurrence of a novel PDGFRB variant and likely pathogenic variant in CASR in an individual with extensive intracranial calcifications and hypocalcaemia. *Clin. Case Rep.*, **6**, 8–13.
20. Nicolas, G., Pottier, C., Charbonnier, C., Guyant-Marechal, L., Le Ber, I., Pariente, J., Labauge, P., Ayrignac, X., Defebvre, L., Maltete, D. et al. (2013) Phenotypic spectrum of probable and genetically-confirmed idiopathic basal ganglia calcification. *Brain*, **136**, 3395–3407.
21. Ramos, E.M., Carecchio, M., Lemos, R., Ferreira, J., Legati, A., Sears, R.L., Hsu, S.C., Panteghini, C., Magistrelli, L., Salsano, E. et al. (2018) Primary brain calcification: an international study reporting novel variants and associated phenotypes. *Eur. J. Hum. Genet.*, **26**, 1462–1477.
22. Arts, F.A., Sciot, R., Brichard, B., Renard, M., de Rocca Serra, A., Dachy, G., Noel, L.A., Velghe, A.I., Galant, C., Debiec-Rychter, M. et al. (2017) PDGFRB gain-of-function mutations in sporadic infantile myofibromatosis. *Hum. Mol. Genet.*, **26**, 1801–1810.
23. Karczewski, K.J., Francioli, L.C., Tiao, G., Cummings, B.B., Alfoldi, J., Wang, Q., Collins, R.L., Laricchia, K.M., Ganna, A., Birnbaum, D.P. et al. (2020) The mutational constraint spectrum quantified from variation in 141,456 humans. *Nature*, **581**, 434–443.
24. Nicolas, G., Wallon, D., Charbonnier, C., Quenez, O., Rousseau, S., Richard, A.C., Rovelet-Lecrux, A., Coutant, S., Le Guennec, K., Bacq, D. et al. (2016) Screening of dementia genes by whole-exome sequencing in early-onset Alzheimer disease: input and lessons. *Eur. J. Hum. Genet.*, **24**, 710–716.
25. Keating, M.T., Harryman, C.C. and Williams, L.T. (1989) Platelet-derived growth factor receptor inducibility is acquired immediately after translation and does not require glycosylation. *J. Biol. Chem.*, **264**, 9129–9132.
26. Pedersen, A.G. and Nielsen, H. (1997) Neural network prediction of translation initiation sites in eukaryotes: perspectives for EST and genome analysis. *Proc. Int. Conf. Intell. Syst. Mol. Biol.*, **5**, 226–233.
27. Petersen, T.N., Brunak, S., von Heijne, G. and Nielsen, H. (2011) SignalP 4.0: discriminating signal peptides from transmembrane regions. *Nat. Methods*, **8**, 785–786.
28. Richards, S., Aziz, N., Bale, S., Bick, D., Das, S., Gastier-Foster, J., Grody, W.W., Hegde, M., Lyon, E., Spector, E. et al. (2015) Standards and guidelines for the interpretation of sequence variants: a joint consensus recommendation of the American College of Medical Genetics and Genomics and the Association for Molecular Pathology. *Genet. Med.*, **17**, 405–424.
29. Nicolas, G., Charbonnier, C., de Lemos, R.R., Richard, A.C., Guillin, O., Wallon, D., Legati, A., Geschwind, D., Coppola, G., Frebourg, T. et al. (2015) Brain calcification process and phenotypes according to age and sex: Lessons from SLC20A2, PDGFB, and PDGFRB mutation carriers. *Am. J. Med. Genet. B Neuropsychiatr. Genet.*, **168**, 586–594.
30. Demoulin, J.B., Uyttenhove, C., Lejeune, D., Mui, A., Groner, B. and Renauld, J.C. (2000) STAT5 activation is required for interleukin-9-dependent growth and transformation of lymphoid cells. *Cancer Res.*, **60**, 3971–3977.
31. Bollaert, E., Johanns, M., Herinckx, G., de Rocca Serra, A., Vandewalle, V.A., Havelange, V., Rider, M.H., Vertommen, D. and Demoulin, J.B. (2018) HBP1 phosphorylation by AKT regulates its transcriptional activity and glioblastoma cell proliferation. *Cell. Signal.*, **44**, 158–170.